Draft version October 8, 2021
Typeset using LaTeX **twocolumn** style in AASTeX63

DNS of Inertial Waves Passing Through Corotation Resonance

V. Skoutnev,[1] A. Astoul (Advisor),[2] and A. Barker (Advisor)[2]

[1] *Department of Astrophysical Sciences and Max Planck Princeton Center, Princeton University, Princeton, NJ 08544, USA*
[2] *Department of Applied Mathematics, School of Mathematics, University of Leeds, Leeds, LS2 9JT, UK*

(Received xx; Revised xx; Accepted xx)

Submitted to

ABSTRACT

We study a model of the propagation of inertial waves into a corotation resonance in a conically and cylindrically differentially rotating convection zone. We focus on the resulting fully non-linear development of a critical layer with sets of direct numerical simulations using the Dedalus code. We first compare linear simulations with theory to verify the code, finding good agreement. Then we perform non-linear simulations where we find that applying linear theory predictions for the evolving mean zonal flow (a quasi-linear approach) does not account for observed reflection and absorption coefficients in either the case when the critical layer is turbulent or the critical layer is laminar but has evolved significantly from its initial flow profile. Thus we find growth of mean flows in the radial direction and nonlinear effects may be important for understanding the efficiency of inertial waves as a tidal dissipation mechanism in planetary and stellar convection zones.

Keywords: Inertial waves–tidal dissipation–critical layers

1. INTRODUCTION

Tidal interactions between a host body and an orbiting, perturbing body can affect the secular evolution of the perturber's rotation and orbit (Ogilvie 2014; Mathis 2015, 2019; Barker 2020). For host bodies with convection zones in their outer regions, such as low mass stars and gaseous giant planets, inertial waves may be excited and play an important role by allowing a net exchange of angular momentum when they are eventually dissipated (Ogilvie & Lin 2007). Propagating inertial waves in a shellular convective region can dissipate either through viscous dissipation (Maas & Lam 1995; Rieutord & Valdettaro 1997), wave breaking, or by absorption if they reach a shear region with a corotation resonance (Baruteau & Rieutord 2013; Guenel et al. 2016), similar to internal gravity waves reaching a critical layer in a stably stratified shear region. In many host bodies, inertial waves dissipation may exceed that of equilibrium tidal dissipation and gravito-inertial wave dissipation in the radiative zone by several order of magnitudes (Ogilvie & Lin 2007). Thus the study of inertial wave dissipation is important for understanding the long term tidal evolution of these astrophysical systems.

We focus on the particular problem of an inertial wave propagating into a velocity shear region in a local model with a corotation resonance and understanding the resulting evolution of the mean flow and the absorption, reflection, and transmission of the wave. A corotation resonance occurs when the horizontal phase velocity, ω/k_x, of a propagating wave matches the local mean flow speed, U (i.e. $U - \omega/k_x = 0$ for a flow in the x-direction). Previous studies of this process investigated the linear theory prediction for absorption, reflection, and transmission coefficients as a function of the relevant dimensionless parameters (Astoul et al. 2021). However, realistically the waves may break and create a turbulent critical layer that may affect properties of the wave propagation, particularly for astrophysically large Reynolds numbers. The mean flow itself will evolve due to the deposition of momentum by the waves and thus additionally affect wave propagation through the region. We implemented a local shearing box model and run sets of direct numerical simulations using the Dedalus code to study these linear and nonlinear processes.

Corresponding author: Valentin Skoutnev
skoutnev@princeton.edu

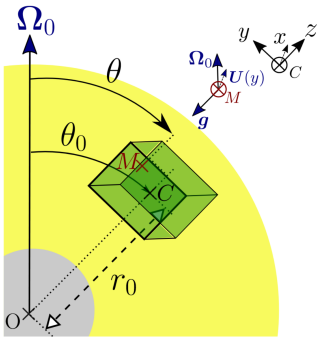

Figure 1. Sketch of local box model embedded in global geometry. Taken from (Astoul et al. 2021).

2. EQUATIONS AND SETUP

2.1. *Equations*

We consider a local shearing box at an angle θ_0 from the pole in a rotating star undergoing conical differential rotation with rotation vector $\vec{\Omega}$ as shown in Figure 1. This setup also captures the case of cylindrical differential rotation for any latitude if the angle $\theta_0 = 0$. The local Cartesian coordinate system sets x in the zonal direction, y in the $-\hat{\theta}_0$ polar direction, and z in the radial direction. Periodic boundary conditions are imposed in the x and z directions, while stress free boundary conditions are imposed in the direction of wave propagation (y direction). Following the derivation in Astoul et al. (2021), we use the non-linear dimensionless fluid equations for the perturbations $\{u, v, w, \rho\}$ around the basic state:

$$D_t u - fv + \tilde{f}w = -\nabla_x P + Re^{-1}\nabla^2 u \quad (1)$$

$$D_t v + fu = -\nabla_y P + Re^{-1}\nabla^2 v + F(x, y, z, t) \quad (2)$$

$$D_t w - \tilde{f}u = -\nabla_z P - \rho + Re^{-1}\nabla^2 w \quad (3)$$

$$D_t \rho = -v\tilde{f}\partial_y U + Re^{-1}\nabla^2 \rho \quad (4)$$

$$\nabla \cdot \vec{u} = 0 \quad (5)$$

where $D_t = \partial_t + \vec{u}\cdot\nabla$, $\vec{u} = (u', v, w)$, $u' = u + U(y)$, and $U(y)$ is the mean flow profile. $F(x, y, z, t)$ is the forcing function localized in the y direction for the inertial waves. In this dimensionalization, $2\vec{\Omega} = 2\Omega(0, \tilde{f}, f) \equiv (0, \tilde{f}, f) \equiv (0, -\sin(\theta_0), \cos(\theta_0))$, where $2\Omega = 1$ is used for the time units.

2.2. *Setup*

We impose a mean shear flow in the region $0 < y < 1$ with $U(y) = U_{max}y$ for the linear profile or $U(y) = U_{max}\tanh((y - 0.5)/0.5)$ for a smoother tanh profile, where U_{max} is a constant parameter. Inertial waves (IWs) with wavevector $\mathbf{k} = (k_x, k_y, k_z)$ are generated in a forcing region that is placed one y-wavelength to the left of the shear region at $y = -2\pi/k_y$. Damping regions are placed to the left of the forcing region and to the right of $y = 1 + 2\pi/k_y$ with a width of $3\pi/k_y$. This way leftwards propagating IWs damp right away while rightward propagating IWs enter the shear region, and any transmitted waves then get dissipated in the right end of the domain. The maximum velocity at the end of the shear region is chosen to be larger than the critical velocity (i.e. horizontal phase speed) of the forced inertial wave, $U_{max} > U_c \equiv \omega/k_x = k_z/(k_x k)$, and thus the critical layer will lie inside the shear region. Lastly, the x and z lengths of the box are a single wavelength of the forced IW, $L_x = 2\pi/k_x$ and $L_z = 2\pi/k_z$ respectively.

3. DIMENSIONLESS PARAMETERS

For comparison with Astoul et al. (2021), the time units are $(2\Omega)^{-1} = 1$ and the length is scaled by the length of the shear region being $0 \le y = y^{(physical)}/L_{shear} \le 1$. For $\theta_0 = 0$ the dimensionless parameters are $\omega/(2\Omega) = k_z/k$, shear Rossby number $R_0 = U_{max}/(L_{shear}\cdot 2\Omega) = \omega/(2\Omega k_x L_{shear} y_0)$, location of corotation resonance y_0, $\alpha_z = k_z/k_x$, $\alpha_y = k_y/k_x$, $k_x = k_x^{(physical)} L_{shear}$ (the choice of k_x sets the ratio λ_x/L_{shear}.), $A/(2\Omega L_{shear})$ (amplitude A of y-velocity forcing), and Ekman $Ek = \nu/(2\Omega L_{shear}^2)$. Note I have followed the definition $0 < y_0 = \omega/(R_0 k_x) = U_c/U_{max} < 1$ for the location of the critical layer. In this notation, the dispersion relation is the no-shear region is

$$\omega = \frac{\alpha_z}{\sqrt{1 + \alpha_z^2 + \alpha_y^2}} \quad (6)$$

$$R_0 = \frac{\omega}{k_x y_0} \quad (7)$$

Assume we want to set a particular ω and R_0 in the simulation with free, dimensionless,"input" parameters y_0, α_z, α_y, and k_x. We have 2 equations and 4 variables. Setting ω determines a relation between α_z and α_y through the dispersion relation. Setting R_0 has some freedom where we can either fix some k_x and then vary y_0 OR fix y_0 and then vary k_x. In order to spread numerical resolution equally along the shear region, the critical layer is always set at the fixed value $y = y_0 = 0.5$ so R_0 is set by varying k_x in the input to the simulation.

4. LINEAR WAVE PROPERTIES

We only consider the case $\theta_0 = 0$ so far, equivalent to the case of cylindrical differential rotation. Outside the forcing and shear regions the plane wave solutions $p = p_0 e^{i(\vec{k}\cdot\vec{x} - \omega t)}$ for $\theta_0 = 0$ are given by:

$$\omega = \pm\frac{k_z}{k} \tag{8}$$

$$u = p\left(\frac{-ik_y - \omega k_x}{1-\omega^2}\right) \tag{9}$$

$$v = p\left(\frac{ik_x - \omega k_y}{1-\omega^2}\right) \tag{10}$$

$$w = p\left(\frac{k_z}{\omega}\right) \tag{11}$$

$$\vec{v}_g = \left(\frac{-k_x k_z}{k^3}, \frac{-k_y k_z}{k^3}, \frac{k_x^2 + k_y^2}{k^3}\right) \tag{12}$$

The forcing region represents a source of IWs, such as launching of IWs from a critical latitude on the edge of a radiative core. We are then studying the subsequent propagation and dissipation of the wave.

By looking at the group velocity, a wave train moving in the direction of $+y$ needs a negative value of $k_y < 0$ for $k_z, \omega > 0$. Thus, an inertial wave approaching a critical layer requires all three components of k and therefore requires a three dimensional simulation (unlike for internal gravity waves which can be simulated in two dimensions, the plane of the horizontal k_h and vertical k_z wavenumbers). $k_y \neq 0$ and $k_z \neq 0$ in order that $v_{g,y} \neq 0$, while $k_x \neq 0$ so that the wave can interact with the shear flow and have a corotation resonance ($\omega - k_x U(y_0) = 0$).

The zonal and radial (vertical for $\theta_0 = 0$) momentum flux transported by the plane wave is given by (supposing $v = v_0 Re[ie^{i(\vec{k}\cdot\vec{x}-\omega t)}]$ as in the simulation):

$$F_{uv}(y,t) = \langle uv \rangle_{xz} = \left(\frac{(\omega^2 - f^2)k_x k_y}{(fk_x)^2 + (\omega k_y)^2}\right)\frac{v_0^2}{2}, \tag{13}$$

$$F_{wv}(y,t) = \langle wv \rangle_{xz} = \left(\frac{(\omega^2 - f^2)k_z k_y}{(fk_x)^2 + (\omega k_y)^2}\right)\frac{v_0^2}{2}. \tag{14}$$

We immediately see that $F_{uv}/F_{wv} = k_x/k_z$, depending on the direction of the wavenumber. Additionally both the zonal and radial components of the mean flow will pick up momentum when the waves dissipate. This would be similar to the internal gravity wave case if the horizontal wave number was not aligned with the mean flow.

An example of the linear case reproduced in the numerical setup is shown in Figure 2 where non-linear terms are present but negligible. We drive a low amplitude wave with $|v_0|/U_c = 0.01$ and after a crossing time of the wave, it is clear that there is no transmission into the region $y > 1$ and some reflection back into $y < 0$ (since the wave shown by the blue curve is slightly out of phase with the analytical incoming wave shown

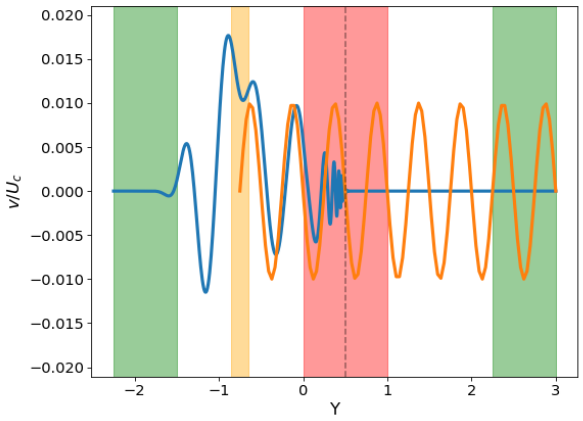

Figure 2. Example of a small amplitude (linear regime) inertial wave driven in the setup after a single wave crossing time based on the y direction group velocity. Yellow is the forcing region, green are the damping regions, red is the shear region, and vertical dashed line at $y = 0.5$ is the corotation resonance location. Blue is the $v(x = 0, y, z = 0, t = 40 * 2\pi/\omega)$ amplitude versus y. Orange is the predicted sine wave propagating to the right if there was no shear region present.

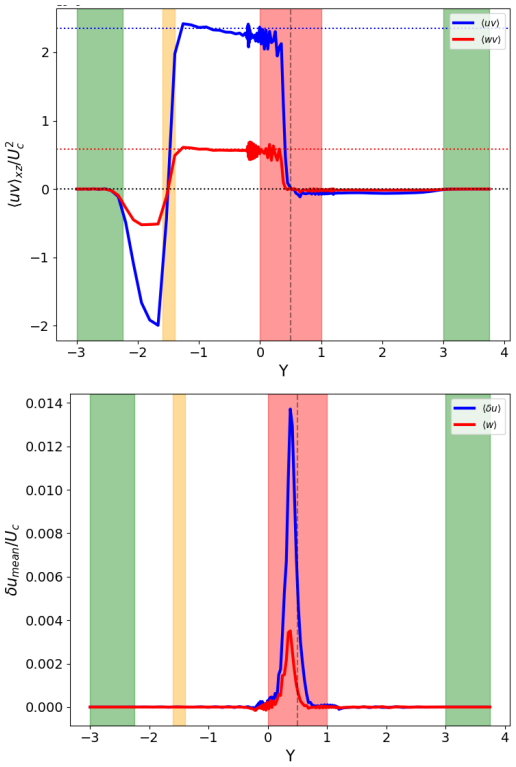

Figure 3. Momentum transport in a simulation with $k_x/k_z = 4$. Top: The XZ averaged wave flux in the y direction of the x momentum (blue) and z momentum (red) components. Dotted lines are analytical predictions. Bottom: Changes in the mean flow profile relative to $t = 0$ in the x (blue) and z (red) directions.

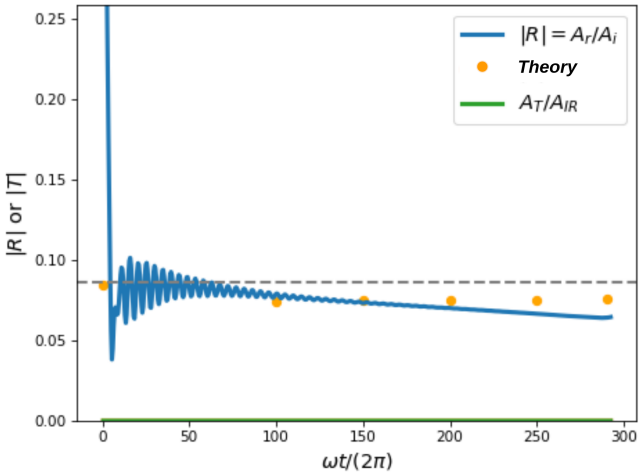

Figure 4. Reflection coefficient vs time in the simulation (blue). Horizontal gray dashed line is linear theory prediction for the initial flow profile. Orange dots are linear theory predictions for the modified x-direction flow profile at that time, $U(y,t)$.

by the orange curve). The reflection and transmission coefficients agree well with the linear prediction (predicted reflection coefficient shown as dashed gray line). Components of the momentum flux and the associated changes in the mean flow components are shown in Figure 3. The entire momentum flux clearly is absorbed in the critical layer for these parameters and the associated mean flow growth of the components is the same ratio as the magnitude of the momentum flux components (i.e. $F_{uv}/F_{wv} = 4$). This is all to say at the linear regime of small amplitude waves early in the simulation agrees well with predictions from linear theory when the mean flow has not changed significantly from its initial linear profile.

5. CRITICAL LAYER DEVELOPMENT AND EVOLUTION

5.1. *Laminar Critical Layer*

While a forcing a small amplitude wave results in a steady state reflection and transmission that agrees with linear theory at early times, the mean flow profile will slowly evolve over longer time scales and leads to a change in the reflection coefficient over time. Figure 4 shows this phenomenon where an early steady state is reached around $\omega t/2\pi = 25$ with a reflection coefficient of ≈ 0.08 that matches linear theory. However, as time progresses $R(t)$ decreases with time down to ≈ 0.06 by the end of the simulation. Does a quasilinear approach predict this behavior? To test this, we substitute the mean x-direction flow profile in the simulation at various times $U(y,t)$ into the linear theory and plot the resulting prediction at the orange dots. The quasilinear correctly predicts that R decreases slightly at first, but it clearly fails to account for further evolution of R.

We presume that this is likely because the linear theory solver only includes a mean $U(y)$ but not the additional $W(y,t) = \langle w(x,y,z,t)\rangle_{xz}$ that is being generated by the $\langle wv\rangle$ component of wave momentum flux, which becomes significant at later times. Thus it appears to be important to consider both the x and z mean flows generated by a flux of inertial waves to understand the evolution of the critical layer already in the laminar case.

5.2. *Turbulent Critical Layer*

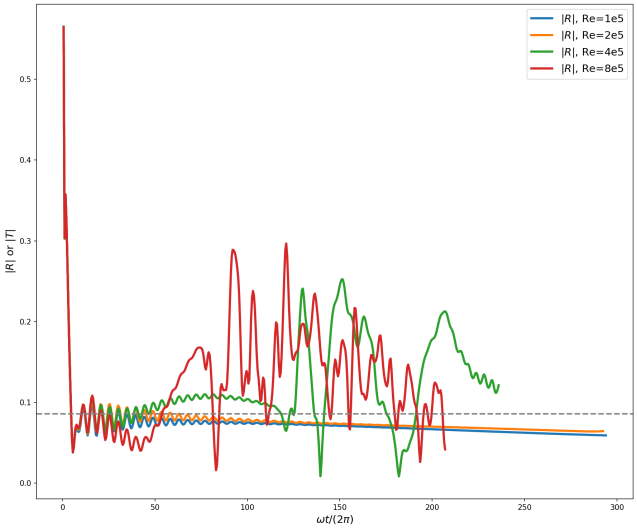

Figure 5. Reflection coefficient vs time. We vary the viscosity in the simulations parameterized by $Re = \nu^{-1}$, while keeping everything else constant. The laminar to turbulent transition clearly occurs between $Re = 2e5$ and $Re = 4e5$.

If either the viscosity is decreased or the amplitude of the wave is increased, then the inertial wave will break right before reaching the corotation resonance and create a turbulent critical layer. This unfortunately requires a large number of modes to resolve the smallest scales, but may just be marginally possible. In Figure 5 we show the reflection coefficient for a series of runs where the viscosity ν (labeled as $Re = \nu^{-1}$) is steadily decreased. It is clear that at some critical viscosity the reflection coefficient suddenly begins to jump and that is when visually the critical layer transitions from laminar to more turbulent (not shown). An even lower viscosity causes the waves to break earlier in time.

The exact criterion for the size of the viscous scales is currently unclear to us so we have so far done a brute force resolution scan in the X and Z modes at the lowest viscosity to see what minimum resolution is needed,

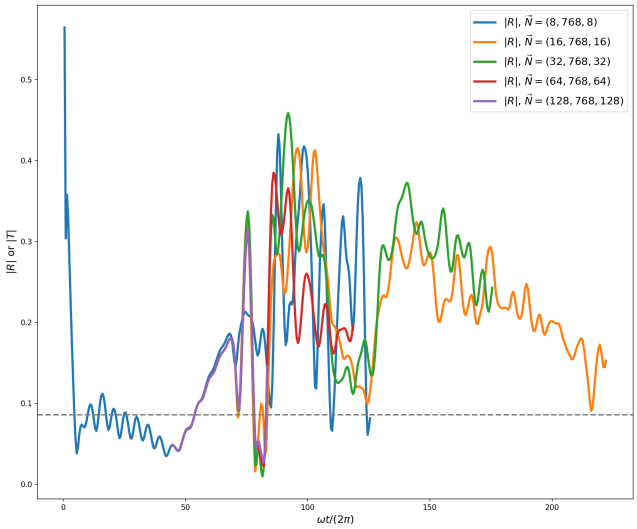

Figure 6. Reflection coefficient vs time. For the highest Reynolds number run in Figure 5 where $Re = 8e5$, we carry out a resolution scan in the number of x and z modes. The notation is $\vec{N} = (N_x, N_y, N_z)$, the number of spectral modes used in each direction. Simulations with more modes are significantly more expensive and therefore were not integrated as in time.

shown in Figure 6. It seems that while a lot of modes are needed in the y-direction, not very many modes are needed in the x and z directions since around 32 modes and above seem to give similar plots of $R(t)$, with later differences probably attributed to chaotic temporal evolution.

In any case, assuming the moderate resolutions in Figure 6 are resolved, it is clear the $R(t)$ on average has significantly increased above it's linear theory prediction and above the more viscous runs with lower Re. Thus is it clear that turbulent critical layers behave significantly differently than laminar ones. This motivates further work to explore turbulent inertial wave critical layers.

6. FUTURE WORK

One remaining goal in the laminar critical layer case is to understand the evolution of the reflection coefficient with time. Over any short time period, the setup should be well approximated by linear theory and it would be interesting to know if the mean flow in the z direction plays an important role here.

In the turbulent critical layer case, there remain many open questions to pursue. What is the criterion for transition between the laminar and turbulent states? In other words, for what amplitudes and viscosities do the waves break in the shear region? Such a criterion would be important for categorizing which state different astrophysical host and companion systems may be in. The obvious next question, is what do turbulent critical layers generally do to the reflection, absorption, and transmission coefficients compared to the linear case? This may require a large parameter scan to see if any patterns emerge.

7. CONCLUSION

In differentially rotating stars or giant planets, inertial waves can be efficiently absorbed in critical layers, which could lead to important tidal dissipation and associated secular evolution of orbiting bodies. We have found that the reflection and absorption properties of waves from these layers is dependent on the wave amplitude and Reynolds number. This motivates further work on this problem to explore the importance of critical layers for tidal dissipation.

ACKNOWLEDGMENTS

This work was initiated during the 2021 Kavli Summer Program in Astrophysics, hosted by the Max Planck Institute for Solar System Research, and funded by the Kavli Foundation.

APPENDIX

A. FORCING FUNCTION RESPONSE IN SHEARLESS REGION $\partial_Y U(Y) = 0$

We need the normalization factor between the forcing amplitude and the amplitude of the resulting wave so that we can have direct control over v_0, the amplitude of the driven wave in the y direction. Following Su et al. (2020), we assume a form $v = v(y)e^{i(k_x x + k_z z - \omega t)}$ for all variables (i.e. the steady state oscillatory response) and solve for the differential equation for $v(y)$. The forcing function is

$$F(x, y, z, t) = e^{i(k_x x + k_z z - \omega t)} \frac{e^{-\frac{y^2}{2\delta^2}}}{\sqrt{2\pi\delta}}. \tag{A1}$$

where δ is the half-width of the forcing region. The equations (now all only a function of y) then are

$$-i\omega u - fv + \tilde{f}w = -ik_x P, \tag{A2}$$
$$-i\omega v + fu = -\partial_y P + F, \tag{A3}$$
$$-i\omega w - \tilde{f}u = -ik_z P, \tag{A4}$$
$$k_x u - i\partial_y v + k_z w = 0. \tag{A5}$$

We need to eliminate P, u in favor of v in order to substitute into the second equation. Incompressibility already gives $w = -(k_x u + k_y v)/k_z$. Some algebra gives:

$$P(y) = \left(\frac{-i(\omega^2 - \widetilde{f^2})\partial_y + i\omega f k_x - f\widetilde{f}k_z}{-\omega(k_x^2 + k_z^2)} \right) v(y) \tag{A6}$$
$$u(y) = \left(\frac{(\omega^2 k_x^2 + \widetilde{f^2}k_z^2)\partial_y + \omega f k_x k_z^2 + if\widetilde{f}k_z^3}{\omega(k_x^2 + k_z^2)(\widetilde{f}k_z - i\omega k_x)} \right) v(y) \tag{A7}$$

Now we can substitute equations A3 with A6 and A7:

$$\left(-i\omega + \frac{\omega f^2 k_x k_z^2 + if^2 \widetilde{f}k_z^3}{\omega(k_x^2 + k_z^2)(\widetilde{f}k_z - i\omega k_x)} \right) v \tag{A8}$$
$$\left(\frac{i\omega f k_x - f\widetilde{f}k_z}{-\omega(k_x^2 + k_z^2)} + \frac{f(\omega^2 k_x^2 + \widetilde{f^2}k_z^2)}{\omega(k_x^2 + k_z^2)(\widetilde{f}k_z - i\omega k_x)} \right) \partial_y v \tag{A9}$$
$$+ \left(\frac{-i(\omega^2 - \widetilde{f^2})}{-\omega(k_x^2 + k_z^2)} \right) \partial_y^2 v = F \tag{A10}$$

Simplifying this gives:

$$\left(\frac{-\omega^2(k_x^2 + k_z^2) + f^2 k_z^2}{\omega^2 - \widetilde{f^2}} \right) v + \left(\frac{-2if\widetilde{f}k_z}{\omega^2 - \widetilde{f^2}} \right) \partial_y v + \partial_y^2 v = \tag{A11}$$
$$\left(\frac{-i\omega(k_x^2 + k_z^2)}{\omega^2 - \widetilde{f^2}} \right) F = CF \tag{A12}$$

This agrees with Eq. 23 in Astoul et al. (2021). The homogeneous solutions (when $F = 0$) are $u_{(1/2)} = e^{ik_{y,(1/2)}y}$, where the $k_{y,(1/2)}$ satisfy the following dispersion relation:

$$-\omega^2(k_x^2 + k_z^2) + f^2 k_z^2 + 2f\widetilde{f}k_z k_y - (\omega^2 - \widetilde{f^2})k_y^2 = 0 \tag{A13}$$

$$k_y = \frac{-2f\widetilde{f}k_z \pm \sqrt{(-2f\widetilde{f}k_z)^2 + 4(-\omega^2(k_x^2 + k_z^2) + f^2 k_z^2)(\omega^2 - \widetilde{f^2})}}{-2(\omega^2 - \widetilde{f^2})} \tag{A14}$$

since ω, k_x, k_z are considered imposed by the forcing. The Wronskian is thus

$$W = i(k_{y,2} - k_{y,1}) = -2i\frac{\sqrt{(-2f\widetilde{f}k_z)^2 + 4(-\omega^2(k_x^2 + k_z^2) + f^2 k_z^2)(\omega^2 - \widetilde{f^2})}}{2(\omega^2 - \widetilde{f^2})} \tag{A15}$$

which nicely simplifies to $W = -2i|k_y|$ in the $\theta_0 = 0$, $\widetilde{f} = 0$ limit, as expected. The steady state particular solution u_p is then given by):

$$v_p = -e^{ik_{y,1}y}\int_0^y \frac{e^{ik_{y,2}y'}}{W}CF(y')dy' + e^{ik_{y,2}y}\int_0^y \frac{e^{ik_{y,1}y'}}{W}CF(y')dy' \tag{A16}$$

Focusing on the left term (and defining $\vec{k}_{y,1/2} = (k_x, k_{y,1/2}, k_z)$)

$$-e^{ik_{y,1}y}\int_0^y \frac{e^{ik_{y,2}y'}}{W}CF(y')dy' = \frac{-AC}{W}e^{i(\vec{k}_1\cdot\vec{x}-\omega t)}\int_0^y \frac{e^{ik_{y,2}y'-\frac{y^2}{2\delta^2}}}{\sqrt{2\pi\delta^2}}dy' \tag{A17}$$

$$= \frac{-AC}{W}e^{i(\vec{k}_1\cdot\vec{x}-\omega t)}e^{-\frac{k_{y,2}^2\delta^2}{2}}\int_0^y \frac{e^{-\frac{(y'+ik_{y,2}\delta^2)^2}{2\delta^2}}}{\sqrt{2\pi\delta^2}}dy' \tag{A18}$$

$$= \frac{-AC}{W}e^{i(\vec{k}_1\cdot\vec{x}-\omega t)}e^{-\frac{k_{y,2}^2\delta^2}{2}}\int_0^{\frac{y+ik_{y,2}\delta^2}{\sqrt{2}\delta}} \frac{e^{-t^2}}{\sqrt{\pi}}dt \tag{A19}$$

$$= \frac{-AC}{2W}e^{i(\vec{k}_1\cdot\vec{x}-\omega t)}e^{-\frac{k_{y,2}^2\delta^2}{2}}\mathrm{erf}\left(\frac{y+ik_{y,2}\delta^2}{\sqrt{2}\delta}\right) \tag{A20}$$

where we have used the definition $\mathrm{erf}(y) = \frac{2}{\sqrt{\pi}}\int_0^y e^{-t^2}dt$. The particular solution is thus given by

$$v_p = \frac{-AC}{2W}e^{i(\vec{k}_1\cdot\vec{x}-\omega t)}e^{-\frac{k_{y,2}^2\delta^2}{2}}\mathrm{erf}\left(\frac{y+ik_{y,2}\delta^2}{\sqrt{2}\delta}\right) + \frac{AC}{2W}e^{i(\vec{k}_2\cdot\vec{x}-\omega t)}e^{-\frac{k_{y,1}^2\delta^2}{2}}\mathrm{erf}\left(\frac{y+ik_{y,1}\delta^2}{\sqrt{2}\delta}\right) \tag{A21}$$

We set A to a give a final velocity amplitude $|v_p(y\to\infty)|/U_c = O(10^{-2})$.

Software: Dedalus (Burns et al. 2020)

REFERENCES

Astoul, A., Park, J., Mathis, S., Baruteau, C., & Gallet, F. 2021, Astronomy & Astrophysics, 647, A144

Barker, A. J. 2020, Monthly Notices of the Royal Astronomical Society, 498, 2270

Baruteau, C., & Rieutord, M. 2013, Journal of Fluid Mechanics, 719, 47

Burns, K. J., Vasil, G. M., Oishi, J. S., Lecoanet, D., & Brown, B. P. 2020, Physical Review Research, 2, 023068

Guenel, M., Baruteau, C., Mathis, S., & Rieutord, M. 2016, Astronomy & Astrophysics, 589, A22

Maas, L. R., & Lam, F.-P. A. 1995, Journal of Fluid Mechanics, 300, 1

Mathis, S. 2015, Astronomy & Astrophysics, 580, L3

—. 2019, EAS Publications Series, 82, 5

Ogilvie, G., & Lin, D. 2007, The Astrophysical Journal, 661, 1180

Ogilvie, G. I. 2014, Annual Review of Astronomy and Astrophysics, 52, 171

Rieutord, M., & Valdettaro, L. 1997, Journal of Fluid Mechanics, 341, 77

Su, Y., Lecoanet, D., & Lai, D. 2020, Monthly Notices of the Royal Astronomical Society, 495, 1239